



Department of Physics & Astronomy
Experimental Particle Physics Group
Kelvin Building, University of Glasgow,
Glasgow, G12 8QQ, Scotland
Telephone: +44 (0)141 339 8855 Fax: +44 (0)141 330 5881

GLAS-PPE/97-09
October 1997

CP Violation and Future ‘B-Factories’

N. H. Brook

Lecture given at “The Actual Problems of Particle Physics”, Gomel, Belarus.

Abstract

This lecture contains a brief introduction to CP violation in the B system before discussing future experimental programmes and their CP reach in the B system.

1 CP Violation in the B-system

Quark mixing in the standard model is described by the Cabibbo-Kobayashi-Maskawa (CKM) matrix [1], eqn(1). Conventionally the u, c and t quarks are unmixed and the mixing is described by the 3×3 V_{CKM} matrix operating on the d, s and b quarks. The matrix elements of V_{CKM} can, in principle, be determined by measuring the charged current coupling to the W^\pm bosons.

$$V_{CKM} \equiv \begin{pmatrix} V_{ud} & V_{us} & V_{ub} \\ V_{cd} & V_{cs} & V_{cb} \\ V_{td} & V_{ts} & V_{tb} \end{pmatrix} \quad (1)$$

The CKM matrix is unitary ie $V_{CKM}^\dagger V_{CKM} = 1$, which leads to 9 unitarity conditions expressed in terms of the matrix elements. There are several (approximate) parameterisations of the CKM matrix, one of the more popular approaches is that of Wolfenstein [2], eqn(2), where the matrix elements are expressed in terms of powers of $\lambda = \sin \theta_c$, where θ_c is the Cabibbo angle. As can be seen from this parameterisation, the 9 complex elements of the matrix can be expressed in terms of 4 independent variables; three real parameters A, λ and ρ and an imaginary part of a complex number, η . The 18 parameters of the CKM matrix can be reduced to 4 because of the unitarity constraints and the arbitrary nature of the relative quark phases [3]. It is the complex phase in the V_{CKM} that leads to CP violation in the standard model.

$$V_{\text{Wolfenstein}} = \begin{pmatrix} 1 - \frac{1}{2}\lambda^2 & \lambda & A\lambda^3(\rho - i\eta) \\ -\lambda & 1 - \frac{1}{2}\lambda^2 & A\lambda^2 \\ A\lambda^3(1 - \rho - i\eta) & -A\lambda^2 & 1 \end{pmatrix} \quad (2)$$

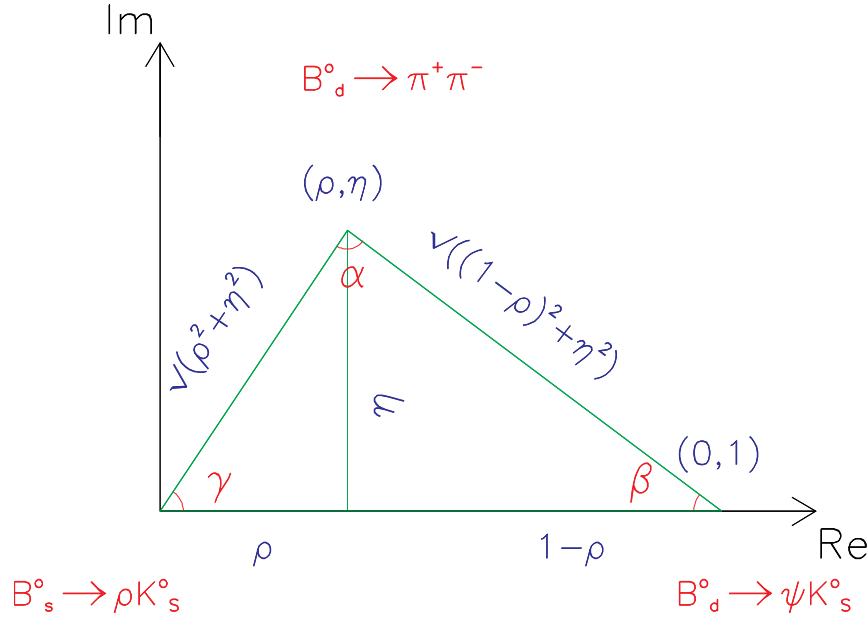
The unitarity condition

$$V_{ud}V_{ub}^* + V_{cd}V_{cb}^* + V_{td}V_{tb}^* = 0$$

is of particular interest since $V_{ud} \simeq V_{tb} \simeq 1$ and $V_{ts}^* \simeq -V_{cb}$. This allows us to depict this condition as a triangle in the complex plane, as shown in fig 1. The angles of the triangle α, β and γ are related to the phase and can be measured in CP violating B -decays.

The non-closure of this triangle ie $\alpha + \beta + \gamma \neq \pi$ would suggest that our understanding of CP violation within the Standard Model was incomplete. Physics beyond the Standard Model can be further investigated, for example, by measuring CP asymmetries in several B decays that depend on the same unitarity angle or studying decays where zero asymmetries are expected in the Standard Model.

CP violation in the B system should be observable through the phenomenon of $B^0 - \bar{B}^0$ mixing, see for example [4]. This $B^0 - \bar{B}^0$ mixing is dominated by box-diagrams with virtual t - quarks, fig 2.



CKM triangle

Figure 1: *The CKM unitarity triangle in the Wolfenstein parameterisation*

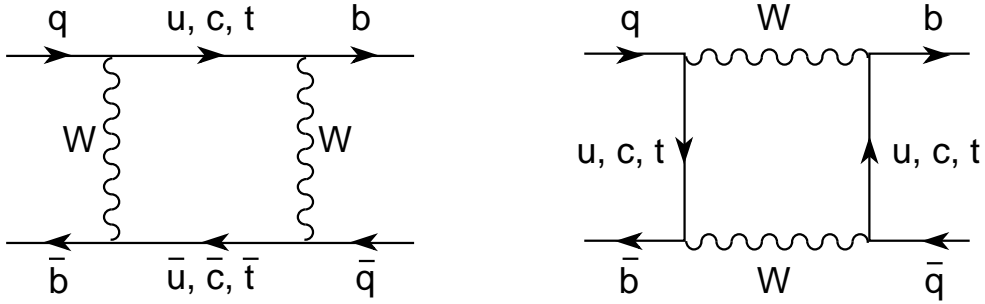


Figure 2: $B^0 - \bar{B}^0$ mixing diagrams.

The following decays

$$\begin{aligned}
 B_d^0 &\rightarrow J/\psi K_s^0 \\
 B_d^0 &\rightarrow \pi^+ \pi^- \\
 B_s^0 &\rightarrow \rho K_s^0
 \end{aligned}
 \tag{3}$$

are into a CP eigenstate. If this is coupled with only a single diagram contributing to the decay, CP asymmetries can be constructed which are directly related to the angles of the unitarity triangle. For example, these conditions occur for the decay mode $B_d^0 \rightarrow J/\psi K_s^0$. Here the number of B_d^0 which decay at time t (where t is expressed in units of lifetime) is proportional to

$$n(t) \propto e^{-t}(1 + \sin 2\beta \sin xt) \tag{4}$$

and the number of \bar{B}_d^0 is proportional to

$$\bar{n}(t) \propto e^{-t}(1 - \sin 2\beta \sin xt) \tag{5}$$

where the mixing parameter, $x = \Delta M/\Gamma \simeq 0.67$, is the ratio of the mass difference of the eigenstates to their decay rate. The CP asymmetry can then be defined as

$$a(t) = \frac{n(t) - \bar{n}(t)}{n(t) + \bar{n}(t)} = \sin 2\beta \sin xt.$$

By integrating eqns. (4) and (5) over time a similar asymmetry can be constructed which is proportional to $\sin 2\beta$. (Although for coherent B production ie the $B\bar{B}$ pair is produced in a definite CP state, this time integrated asymmetry is zero.) In addition this channel is experimentally very promising because of the dilepton decay of the J/ψ . Unfortunately additional decay diagrams contribute to the other channels listed in eqn(3) so there is no longer a complete cancellation of the hadronic matrix elements in the CP asymmetry. The $B_d^0 \rightarrow \pi^+\pi^-$ channel, which is dependent on the angle α is predicted to have large hadronic corrections from ‘penguin’ diagrams, fig. 3. The $B_s^0 \rightarrow \rho K_s^0$ (dependent on the angle γ) also has additional hadronic contributions but, in addition, suffers from a very low branching fraction. Fortunately there are, of course, many other channels which can be used to measure CP violation, eg see ref. [5].

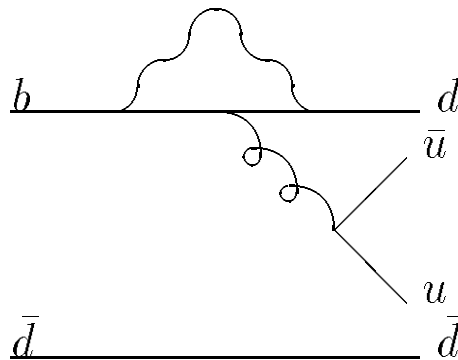


Figure 3: ‘Penguin’ contribution to $B_d^0 \rightarrow \pi^+\pi^-$ decay

2 B-Production Facilities

Because of the small visible branching ratios of decays to CP eigenstates, $\mathcal{O}(10^{-5})$, a large number of B meson must be produced in order to study CP violation in the B system. There are two complimentary ways to achieve the necessary large number of B mesons. The first is at e^+e^- colliders at centre of mass energy of 10 GeV to produce the $\Upsilon(4S)$ which then decays to two B mesons. Alternatively high energy hadron machines, where there is a large cross section for $b\bar{b}$ production, can be used to produce the B mesons. The pros and cons of the various approaches are discussed in this sections.

2.1 e^+e^- Colliders

B meson production via e^+e^- colliders is being pursued at laboratories in the United States (Cornell and SLAC) and Japan (KEK). The luminosity at these machines is of the $\mathcal{O}(10^{33}) \text{ cm}^{-2}\text{s}^{-1}$ which is equivalent to approximately 4 $b\bar{b}$ pairs produced every second. Because the B mesons produced from the decay of $\Upsilon(4S)$ are coherent it is necessary to be able to measure the time separation between the two B ’s in order to measure the CP asymmetry through $B^0 - \bar{B}^0$ mixing. To give the $\Upsilon(4S)$ sufficient boost to allow the two B^0 decay vertices to be reconstructed and

thus the distance between the two B mesons to be measured, the beam energies at SLAC and KEK are asymmetric. The Cornell B-facility has symmetric beam energies and will be unable to measure CP asymmetry through $B^0 - \bar{B}^0$ mixing though there are possibilities to measure CP violation through the decays of charged B 's. The KEK and SLAC facilities are asymmetric with $e^- (e^+)$ energies of 3.5 GeV (8 GeV) and 3.1 GeV (9 GeV) respectively. The need for the large luminosity and the asymmetric beam energies poses great challenges on the machine design. The advantages of this approach is the very clean production environment of the 2 B mesons, with no underlying event from which to extract the signal. By running at the mass of $\Upsilon(4S)$ it is not possible, simply by kinematic constraints, to study the B_s system. In order to study the B_s system the machine can be operated with energies at the mass of $\Upsilon(5S)$ but the cross sections are much smaller.

2.2 Hadron Colliders

The high energy hadron machines, Tevatron and HERA (in fixed target mode with a wire target inserted into the proton beam halo), are already producing large numbers of B mesons. The LHC will produce even greater numbers. At the Tevatron the $b\bar{b}$ production rate is $\mathcal{O}(10^4)$ Hz and at LHC it will be $\mathcal{O}(10^5)$ Hz compared to the $\simeq 4$ Hz at SLAC and KEK. The problem in this approach is achieving high enough reconstruction and tagging efficiencies in order to extract a sufficient number of B 's to measure CP violation. The LHC has an additional benefit over the Tevatron and HERA because with the increasing centre of mass energy the ratio of the $b\bar{b}$ cross section over the total inelastic cross section also increases. All the hadron machines also have the advantage that they can study B_s mesons.

3 The Experiments

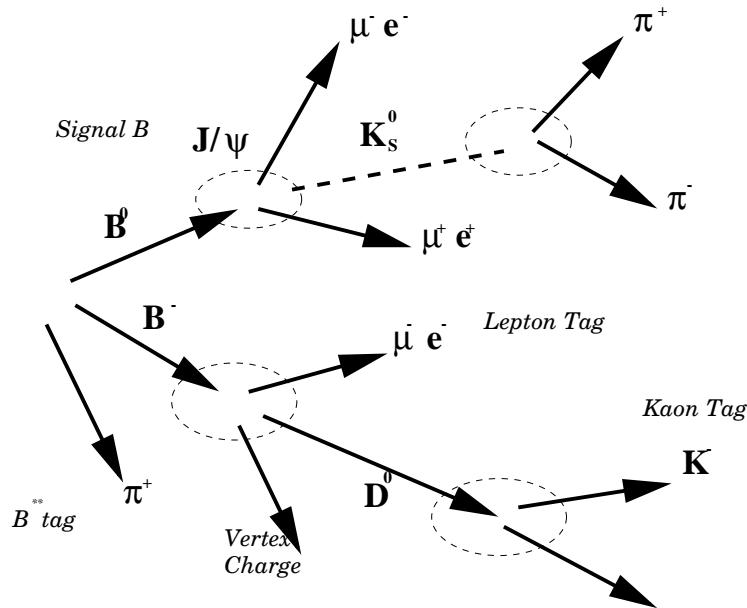


Figure 4: *Example of B tagging.*

To measure CP violation it is not only necessary to measure the decay of the B meson but also to tag its initial flavour via the decay of the accompanying B , as shown schematically in fig. 4. The generic detector requirements for an experiment to study B decays are that it

has good resolution on measuring the decay time and the mass of decayed B mesons and has particle identification to allow a good initial flavour tag of the B meson. The characteristics of the detectors designed to study CP violation are discussed below.

3.1 BELLE

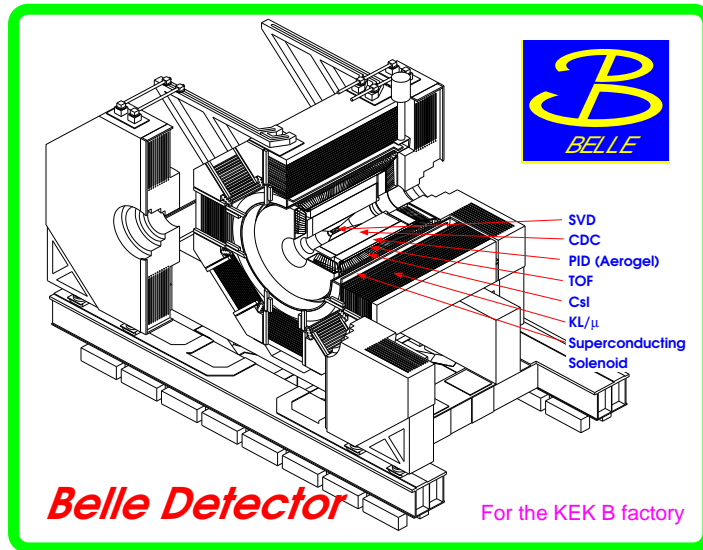


Figure 5: *Schematic of the BELLE detector at the KEK B factory.*

The BELLE detector [6] is the experimental apparatus being designed for the KEK B factory. A schematic of the detector is shown in figure 5. The detector consists of a silicon vertex detector (SVD) situated just outside the beampipe. Surrounding that there is a cylindrical wire drift chamber (CDC) that measures charged tracks which extends to a radius of 90 cm. Particle identification is provided by dE/dx measurements in the CDC, and aerogel Čerenkov counter and time of flight (TOF) arrays situated radially around the CDC. Inside the superconducting solenoid is an electromagnetic calorimeter manufactured from CsI(Tl) crystals. The iron return yoke of the 1.5 Tesla solenoid is interspersed with arrays of detectors for measuring muons and K_L^0 mesons. The design of the equivalent detector, BaBar, at the SLAC B factory is discussed in ref. [7].

3.2 HERA-B

To guarantee the observation of standard model CP violation in B decays (after folding in the detector efficiencies), interactions at the HERA-B detector have to occur approximately 4 times for every one of the 10 MHz bunch crossings of the HERA machine. The HERA-B experiment is essentially a fixed target experiment with a wire target in the beam halo [8]. A schematic of the HERA-B spectrometer is shown in fig. 6. It has a single dipole momentum spectrometer situated 4.5 m downstream of the target. Directly downstream of the target wires, but before the magnet, there is a silicon vertex detector of length of ~ 2 m. The main tracking system uses a variety of technologies dependent on the distance away from the beam (Si-strips, microstrip gas counters and honeycomb-drift chambers at ever increasing radii from the beam.) This is followed by a ring imaging Čerenkov (RICH) detector to tag the charged kaon and a transition radiation detector to improve electron identification. There are additional large tracking

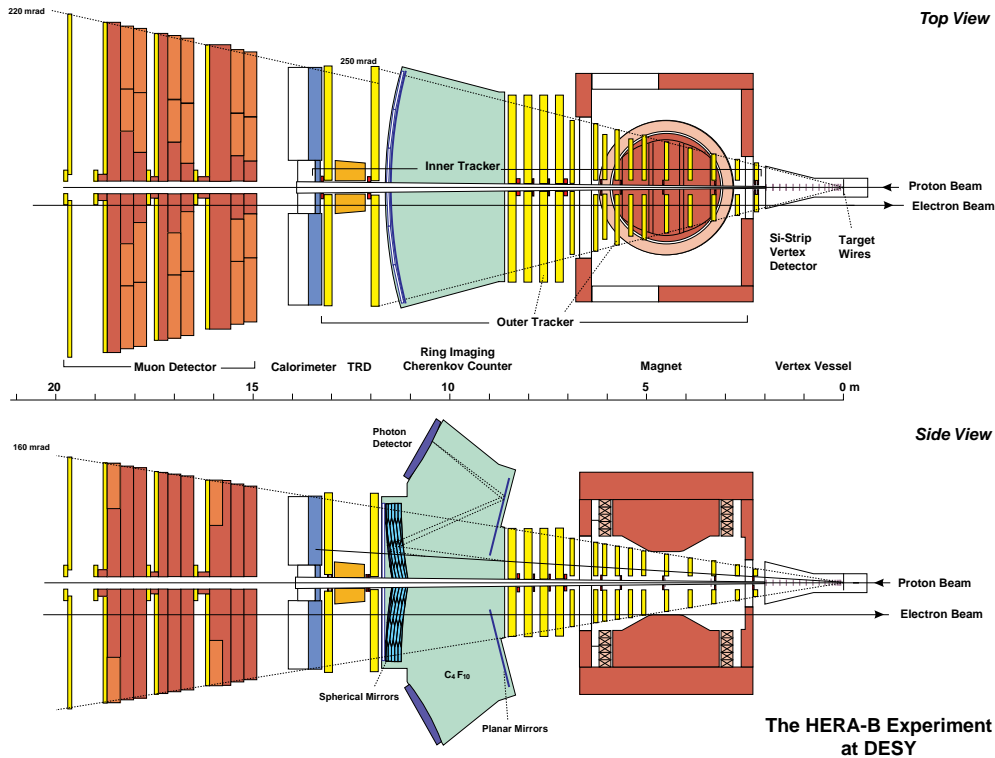


Figure 6: Schematic of the HERA-B detector at DESY.

chambers immediately behind the RICH and in front of the calorimeter. The electromagnetic calorimetry is designed to use Lead/Scintillator and Tungsten/Scintillator. This is followed by a conventional muon system with four chamber layers at various depths in the absorber. The muon chambers are essential for the triggering of HERA-B when the J/ψ decays to two muons.

3.3 CDF and D0

There is already a very active B physics program at the CDF detector at the Tevatron. The B meson lifetime measurements, fig. 7, are already competitive with those of the combined LEP experiments. This proves that it is possible to extract B physics from the hostile experimental environment of the hadron colliders. Both CDF [9] and D0 [10] are hoping to exploit the Tevatron upgrade (RUN II in 1999) to study CP violation in the B -system.

CDF are proposing a new tracking system for Run II, fig. 8. At large radii they will have a central outer tracker (COT) of an open drift chamber design. Inside this component there is a silicon inner tracker comprising of two components: a micro-vertex detector (SVX II) at very small radii and two additional layers of silicon at intermediate radii. The current forward calorimetry is going to be replaced with a new scintillating tile plug calorimeter. New chambers will be added to the current muon system to close gaps in the azimuthal acceptance and the forward acceptance will be improved. The trigger will also be upgraded to allow track finding at level-1 and the ability to trigger on large impact parameter tracks at level-2.

A major element of the D0 upgrade is their new inner tracking system which will be located inside a new 2 Tesla superconducting solenoid. It will consist of an inner silicon vertex detector, surrounded by eight superlayers of scintillating fibre tracker. In the forward region, on the face of the end calorimeter cryostats, and in the central region, located between the solenoid and the inner radius of the calorimeter cryostat, a scintillator based pre-shower detector will be installed. The trigger upgrades will include tracking triggers at level-1 and an upgraded level-2

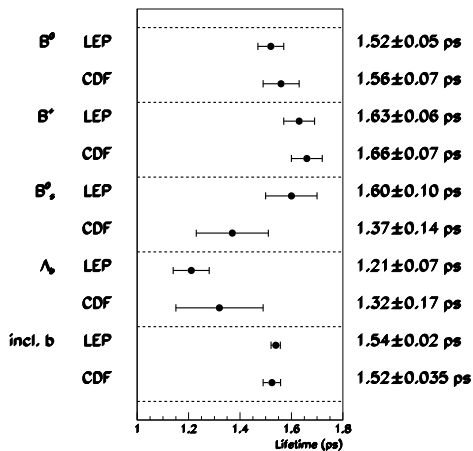


Figure 7: A comparison of CDF and LEP B meson lifetime measurements.

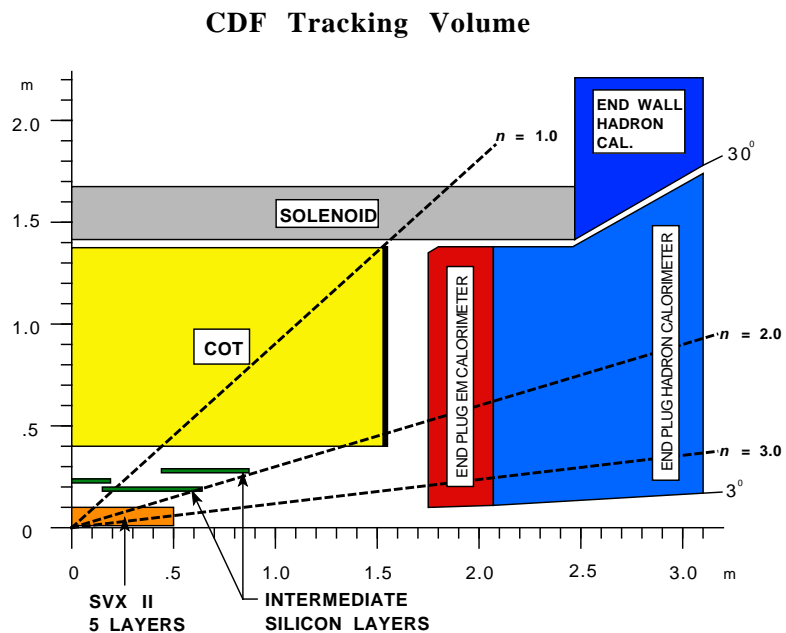


Figure 8: Longitudinal View of the CDF II Tracking System.

muon triggers.

3.4 ATLAS and CMS

The ATLAS [11] and CMS [12] detectors at the LHC are optimised for high luminosity physics. But initial low luminosity running will allow these general purpose detectors to be used for B physics. Both detectors are installing silicon vertex detectors close to the beampipe. More detailed discussion of these detectors and their physics performance can be found elsewhere in these proceedings [13].

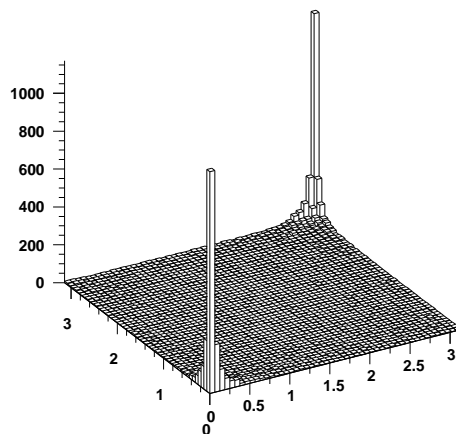


Figure 9: Production angle of B vs. angle of \bar{B} in the laboratory (in units of rad.) at LHC calculated using the the PYTHIA Monte Carlo generator [14].

3.5 LHC-B

At high energy hadron colliders the produced B and \bar{B} mesons are correlated in the forward direction (ie close to the proton beam direction). Figure 9 shows the angular distribution of the $B\bar{B}$ mesons in the laboratory frame at LHC. This is due to the relatively low mass production of b quark pairs at collider energies. This production mechanism lends itself to dedicated experiments that are of a forward, planar design, reminiscent of those used in fixed target experiments.

Such an experiment, LHC-B, has been proposed for the LHC [15]. Its layout is shown in figure 10. LHC-B is a forward single-dipole spectrometer. It consists of a silicon microvertex detector, a tracking system, aerogel and gas RICH detectors, electromagnetic and hadronic calorimeter and a muon filter. LHC-B will be allowed to run with a defocused beam in their interaction area which would give a nominal running luminosity $\mathcal{L} = 1.5 \times 10^{32} \text{ cm}^{-2}\text{s}^{-1}$.

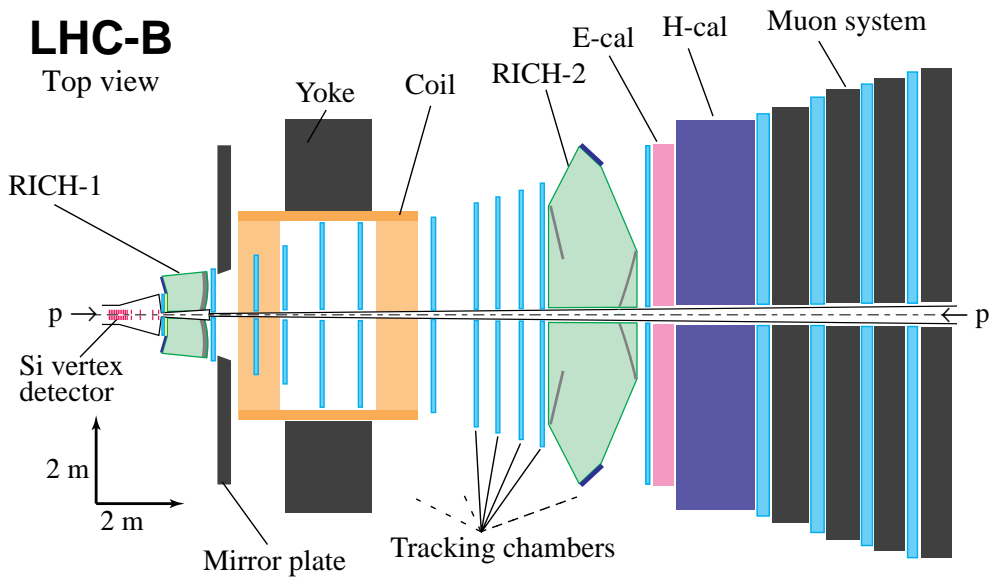


Figure 10: *Top view of the LHC-B detector*

3.6 BTeV

Recently a similarly motivated experiment (BTeV) has submitted a expression of interest at Fermilab [16]. The schematic layout of the BTeV proposal is shown in figure 11. The baseline description of the detector has a dipole magnet centred on the interaction region, thus providing the basis for a two-arm spectrometer. A vertex pixel detector (inside the magnetic field) provides high resolution tracking near the interaction. The baseline design has seven downstream tracker stations of straw tubes along both arms of the spectrometer. For identification of electromagnetic final states and kaons there is electromagnetic calorimetry and a RICH detector respectively, with a toroidal magnetic detector for muon identification and measurement. The BTeV detector relies heavily on the vertex detector for triggering of the B events.

3.7 Experimental Recap

Table 1 summarises the experiments discussed previously in this section. The SLAC and KEK B factories are due to take first data before the turn of the century. Though it is important to remember that new accelerators often take 2-3 years to reach their design goals. HERA-B

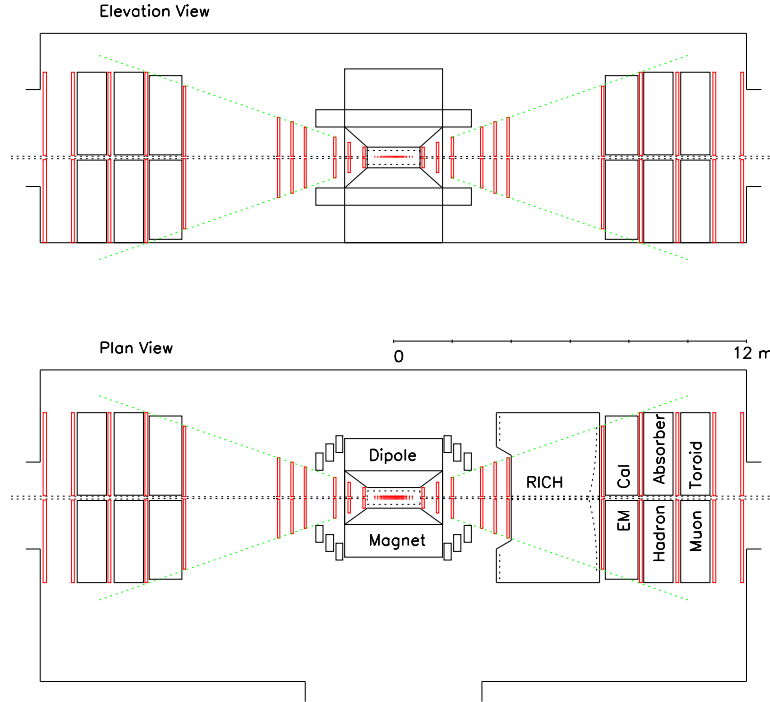


Figure 11: *Schematic Layout of the BTeV detector*

is already partially instrumented and is already taking data in situ in order to debug and test some of their detector components. They have already achieved the multiple interaction per bunch crossing that is necessary to meet their design considerations. CDF and D0, like the experiments at the e^+e^- machines, are due to take data again before the end of the century. With their already proven track record in B physics they should be in a good position to be the first to observe CP violation in the B system. Beyond that LHC-B and BTeV (in addition ATLAS and CMS) should be in a good position to further test and even overconstrain the unitarity triangle of CP violation in the standard model and perhaps any new physics beyond.

Experiment	Machine	Collision Type	Centre of Mass Energy	Start
CDF/D0	Tevatron	$p\bar{p}$	2TeV	1999
ATLAS/CMS	LHC	pp	14TeV	2005
HERA-B	HERA	pN	40GeV	1998
BaBar	PEP-II	e^+e^-	$\Upsilon(4S)$	1999
BELLE	KEKB	e^+e^-	$\Upsilon(4S)$	1999
BTeV	Tevatron	$p\bar{p}$	2TeV	2002
LHC-B	LHC	pp	14TeV	2005

Table 1: *Properties of the experiments*

4 CP Reach

In table 2 is a comparison of the statistical precision that BaBar (and BELLE) and HERA-B claim can be achieved in measuring $\sin 2\alpha$ and $\sin 2\beta$ for one year's running at design luminosity. The two experiments are comparable in the $B^0 \rightarrow J/\Psi K_s^0$ channel, but there are other channels that BaBar can use, because of the clean event environment, to extract the angle α . For measuring $\sin 2\beta$ at first glance the two experiments are again comparable, but the figures quoted in the table are for zero background. HERA-B will have a background in $B^0 \rightarrow \pi^+\pi^-$ channel and the quoted figures need to be modified by a factor $\sqrt{1+B/S}$ where B/S is the ratio of background to signal. It is thought that a value of $B/S < 1$ can be achieved [17].

Decay Channel	BaBar	HERA-B
$J/\Psi K_s^0$ evts		
$\Delta \sin 2\beta$	± 0.10	± 0.13
All channels		
$\Delta \sin 2\beta$	± 0.06	± 0.13
$\pi^+\pi^-$		
$\Delta \sin 2\alpha$	± 0.20	± 0.14
$\rho^\pm\pi^\pm$		
$\Delta \sin 2\alpha$	± 0.11	
All channels		
$\Delta \sin 2\alpha$	± 0.085	± 0.14

Table 2: A comparison of the experimental accuracy of the BaBar and HERA-B experiments

Table 3 reviews the accuracy that the experiments at hadron colliders hope to achieve from 10^7 seconds running. Besides the accuracy on $\sin(2\alpha)$ and $\sin(2\beta)$, the measurement precision and upper limit of γ and x_s (comparable to x in the B_d system) are listed, which need the B_s mesons to be detected and tagged. The figures show that the dedicated experiment at the LHC, LHC-B, has by far the best reach in measuring the parameters of CP violation. It is also worth noting that the performance of the Tevatron general purpose detectors are comparable to result expected from HERA-B and thus the $e^+e^- B$ factories. (It should be noted though the clean experimental environment in e^+e^- allows them to make a more complete study of rare B -decays.)

	CDF/D0	HERA-B	ATLAS/CMS	LHC-B	BTeV
$\Delta \sin(2\alpha)$	~ 0.10	~ 0.14	0.10/0.07	0.039	0.1
$\Delta \sin(2\beta)$	~ 0.10	~ 0.13	0.02/0.07	0.023	0.042
$\Delta\gamma$				6 – 16°	
x_s		≤ 17	≤ 34	≤ 55	≤ 30

Table 3: A comparison of the experimental accuracy and reach of the experiments at hadron facilities. All but BTeV data taken from ref. [18]. BTeV limits from their EoI [16].

5 Conclusions

There is a strong program of future experiments planning to study CP violation in the B system. The first generation experiments start taking data in the next few years. Second

generation experiments are already being planned to extend the measurement of CP violation. The experiments will over constrain the unitarity triangle and perhaps indicate new physics beyond the Standard Model.

References

- [1] M. Kobayashi and T. Maskawa, *Prog. Theor. Phys.* 49 (1973) 652.
- [2] L. Wolfenstein, *Phys. Rev. Lett.* 51 (1983) 1945.
- [3] J. L. Rosner, ‘The Cabibbo-Kobayashi-Maskawa Matrix’, in *B Decays* (World Scientific), ed. S. Stone.
- [4] Y. Nir and H. R. Quinn, ‘Theory of CP Violation in *B* Decays’, in *B Decays* (World Scientific), ed. S. Stone.
- [5] I. Dunietz, ‘CP Violation with Additional *B* Decays’, in *B Decays* (World Scientific), ed. S. Stone.
- [6] BELLE Collab., M. T. Cheng et al., Technical Design Report, KEK-Report 95-1.
- [7] BaBar Collab., D. Boutigny et al., Technical Design Report, SLAC-R-95-457.
- [8] HERA-B Collab., E. Hartouni et al., Technical Design Report, DESY-PRC-95/01.
- [9] CDF Collab., R. Blair et al., The CDF II Detector Technical Design Report, FERMILAB-Pub-96/390-E.
- [10] D0 Collab., The D0 Upgrade: The Detector and its Physics, Fermilab Pub-96/357-E.
- [11] ATLAS Collab., W. W. Armstrong et al., ATLAS Technical Proposal, CERN/LHCC/94-43.
- [12] CMS Collab., G. L. Bayatian et al., CMS Technical Proposal, CERN/LHCC/94-38.
- [13] I. Vichou, ‘Physics with the ATLAS detector at LHC’, to appear in these proceedings;
I. Efthymiopoulos, ‘Overview of the ATLAS Detector at LHC’, to appear in these proceedings;
G. Snow, ‘CMS General Overview and Physics Performance’, to appear in these proceedings;
R. Ribeiro, ‘The Tracking System of CMS’, to appear in these proceedings;
D. Barney, ‘The CMS Crystal Calorimeter’, to appear in these proceedings.
- [14] T. Sjöstrand, *Computer Physics Commun.* 39 (1986) 347;
H.-U. Bengtsson and T. Sjöstrand, *Computer Physics Commun.* 46 (1987) 43.
- [15] LHC-B Collab., K. Kirsebom et al., LHC-B Letter of Intent, CERN/LHCC 95-5.
- [16] BTeV Collab., A. Santoro et al., BTeV: An Expression of Interest for a Heavy Quark Program at C0, BTeV-pub-97/2
- [17] I. Abt, *Proceedings of Beauty’96*, *Nucl. Instr. Meth.* A384 (1996), 113.
- [18] *Proceedings of Beauty’96*, *Nucl. Instr. Meth.* A384 (1996).